

# High Performance 1.3 $\mu\text{m}$ Aluminum-Free Quantum Dot Lasers Grown by MOCVD

Lei Wang, Hongwei Zhao, Bei Shi, Sergio Pinna, Simone Suran Brunelli, Fengqiao Sang, Bowen Song, Jonathan Klamkin

*Electrical and Computer Engineering Department, University of California, Santa Barbara, CA 93106 USA  
leiwang@ucsb.edu*

**Abstract:** MOCVD grown aluminum-free quantum dot lasers have been demonstrated with a maximum wall-plug efficiency of 30%, a lowest threshold current of 8 mA, and a maximum single-facet output power of 200 mW. © 2020 The Author(s)

**OCIS codes:** (130.0130) Integrated optics; (250.5590) Quantum well, -wire and -dot devices; (140.5960) Semiconductor lasers

## 1. Introduction

Owing to the benefits of three-dimensional carrier confinement, self-organized indium arsenide (InAs)/gallium arsenide (GaAs) quantum dot (QD) lasers have undergone significant development and have demonstrated low threshold current density [1], high characteristic temperature [2], and high wall-plug efficiency (WPE) [3]. QD lasers, therefore, are considered superior to their quantum well (QW) counterpart, especially for the fast-growing data communication market where low cost, low energy consumption, and high temperature stability lasers are desirable [3]. Many of the reported high performance QD lasers were grown by molecular beam epitaxy (MBE) and utilize aluminum gallium arsenide (AlGaAs) for the cladding layers [4]. For large-volume production, however, metal organic chemical vapor deposition (MOCVD) is considered the industry standard epitaxy technology. MOCVD additionally allows for selective area and nonplanar growth, which are critical for realizing single-frequency monolithic laser sources and for integration into a silicon photonics (SiPh) process. For MOCVD, AlGaAs typically requires high growth temperature (on the order or above 700 °C). For the upper cladding growth, such a high growth temperature would alter the as-grown QDs and result in a strong blueshift for the QD emission. Alternatively, GaAs lattice matched indium gallium phosphide (InGaP) has a suitable refractive index and bandgap and can be grown by MOCVD at a temperature as low as 500°C [5]. The InGaP/GaAs material system is also beneficial for avoiding aluminum-containing compounds and potential oxidation during fabrication. This approach is therefore especially beneficial for devices that require regrowth over gratings such as distributed feedback (DFB) lasers or more advanced photonic integrated circuits (PICs).

The primary challenges for MOCVD to realize QD lasers with InGaP cladding layers include the difficulty in controlling the QD uniformity due to complex growth dynamics, and the phase separation issue associated with thick layer growth of InGaP especially on (001) GaAs. In this work, we have demonstrated high performance MOCVD grown aluminum-free QD lasers on semi-insulating (001) GaAs. Fabricated Fabry-Perot (FP) lasers demonstrate a maximum WPE of 30%, a lowest threshold current of 8 mA, and a maximum single-facet output power of 200 mW. For datacenter interconnects, these results are promising for providing efficient lasers that can serve as a remote optical source, be hybrid integrated with SiPh circuits, or be monolithically integrated on silicon owing to the lower sensitivity to defects attributed to QDs [4, 6].

## 2. Material growth and device fabrication

The QD laser material was grown on (001) semi-insulating GaAs using a horizontal reactor MOCVD system. The layer structure is summarized in Fig. 1(a). The active region contains a five-layer undoped dots-in-a-well (DWELL) structure [6]. Two 75-nm-thick GaAs layers surrounding the active region create a separate confinement heterostructure. Lattice-matched InGaP is utilized for the lower n-doped and upper p-doped cladding layers, and both are 1.3  $\mu\text{m}$  thick. The n-doped InGaP is grown at a temperature of 580°C to yield a smooth surface, and the p-doped InGaP is grown at 550°C to preserve the morphology of the QDs. The ohmic contact layers are highly doped n-GaAs and p-GaAs. A photoluminescence (PL) spectrum measured at room temperature (RT) with a pump intensity of 9 W/cm<sup>2</sup> is shown in Fig. 1(b), where the peak wavelength is approximately 1270 nm and the full width at half maximum (FWHM) is approximately 110 nm. The inset of Fig. 1 (b) is a 1  $\mu\text{m}$   $\times$  1  $\mu\text{m}$  atomic force microscope (AFM) image of QDs grown under the same conditions as for the laser. This image reveals a dot density

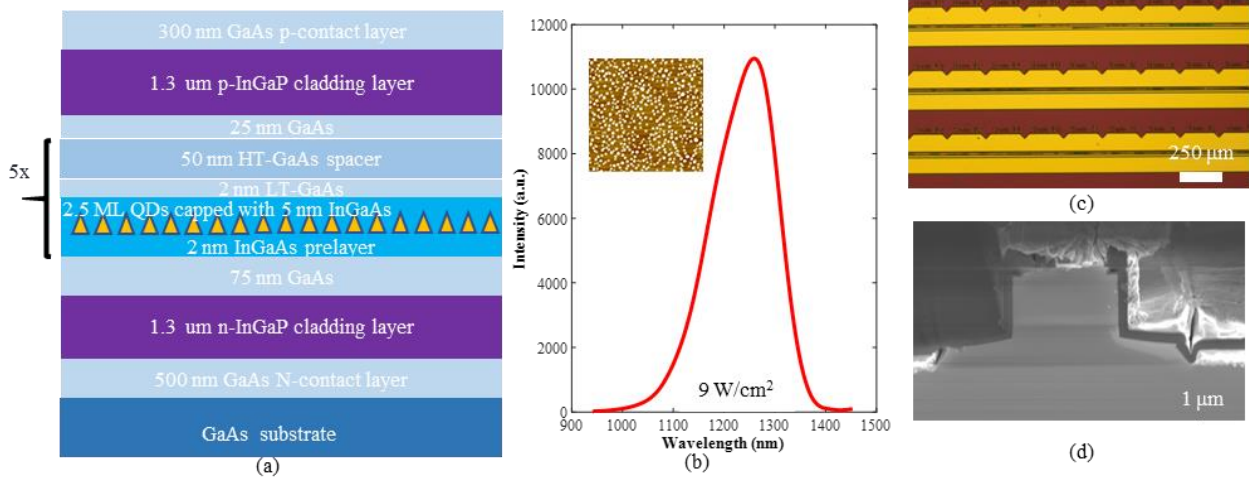


Fig. 1. (a) Layer structure for the QD laser. (b) PL spectrum of laser structure with AFM image inset for QDs grown under the same conditions as for the laser. (c) Optical microscope image of laser bar on GaAs prior to facet cleaving. (d) SEM image of 3-μm-wide ridge cleaved laser facet.

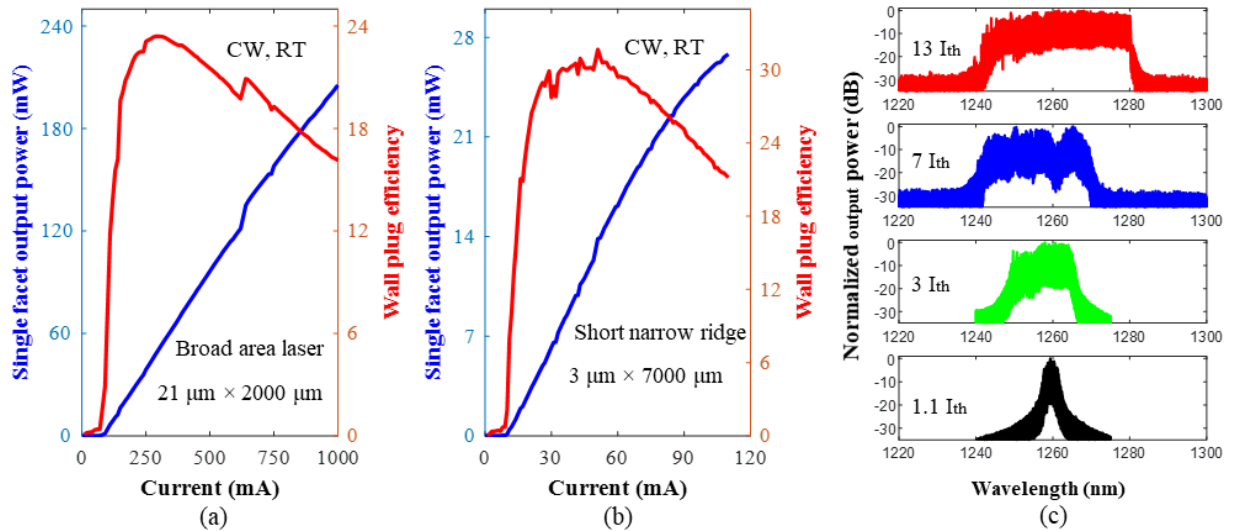


Fig. 2. Light-current curve at RT for (a) a representative broad area laser and (b) a representative narrow ridge laser. (c) Lasing spectra of the broad area laser at various above-threshold current injection levels.

of  $5.5 \times 10^{10} \text{ cm}^{-2}$ . Deep ridge waveguides were defined by inductively coupled plasma reactive ion etching (ICP-RIE). For p- and n-metal contacts, Ti/Pt/Au and Ni/AuGe/Ni/Au were deposited by electron-beam evaporation. A 2-μm-thick Au film was further deposited for probe metal. Figure 1(c) shows an optical microscope image of fabricated laser bars prior to facet cleaving and Fig. 2(d) shows a scanning electron microscope (SEM) image of a 4-μm-wide cleaved laser facet.

### 3. Laser characterization

The laser devices were mounted on aluminum nitride ceramic carriers for characterization. All of the measurements presented were carried out under continuous wave (CW) operation and at RT. The laser facets were not coated. Figure 2(a) and 2(b) show the light-current characteristics for a representative broad area laser (21 μm × 2000 μm) and a narrow ridge laser (3 μm × 700 μm). The maximum WPE for these lasers are 23% and 30%, respectively. The maximum single facet output power of the broad area laser is greater than 200 mW (the measurement is limited by the 1 A maximum for the current source used). The threshold current ( $I_{th}$ ) for the narrow ridge laser is approximately 8 mA (threshold current density,  $J_{th} = 130 \text{ A/cm}^2$ ). These measurement results indicate that the QD lasers are highly

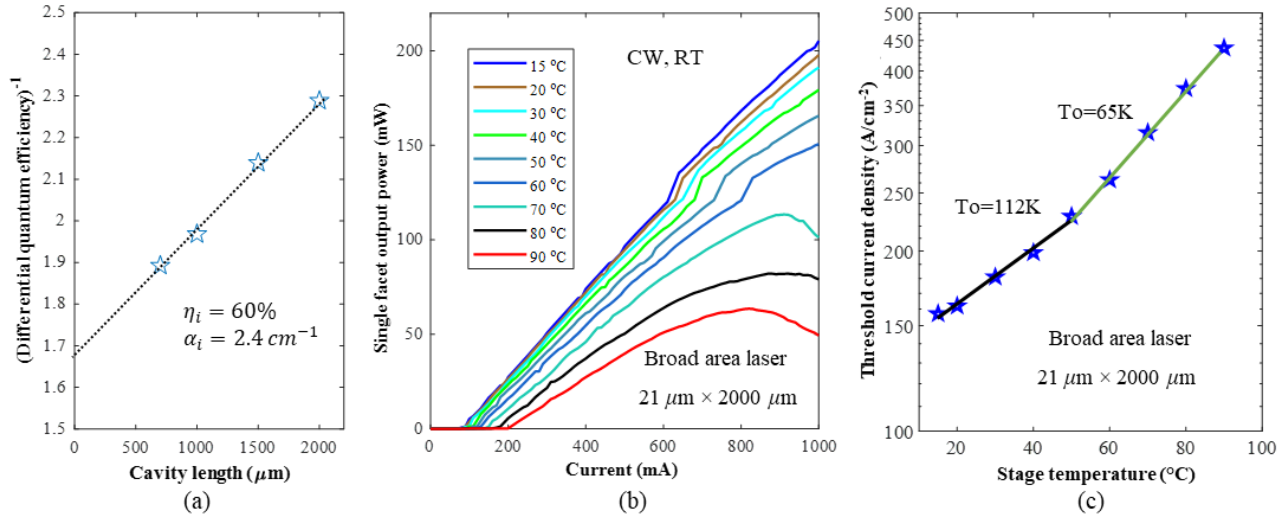


Fig. 3. (a) Reciprocal of measured differential efficiency versus cavity length for the 3- $\mu\text{m}$ -wide lasers. (b) Light-current characteristics for the broad area laser at various stage temperatures. (c) Threshold current density of the broad area laser at various stage temperatures.

efficient and suitable for low-power optical interconnect applications. Figure 2(c) shows the lasing spectra for the broad area laser ( $21 \mu\text{m} \times 2000 \mu\text{m}$ ) at various above-threshold current levels. Even under high injection level ( $13 I_{\text{th}}$ ), there is no apparent excited state lasing (expected at a wavelength of approximately  $1.2 \mu\text{m}$ ). The maximum bandwidth of the lasing spectra is approximately 30 nm, which indicates the potential to develop broadband comb laser sources with this QD material. The measured differential efficiency of the 3- $\mu\text{m}$ -wide ridge lasers as a function of cavity length is shown in Fig. 3(a). The injection efficiency  $\eta_i$  and the internal loss  $\alpha_i$  were extracted to be approximately 60% and  $2.4 \text{ cm}^{-1}$ . The thermal performance was also characterized for the broad area laser. Figure 3(b) shows the light-current curves at various stage temperatures. The QD laser continues to exhibit high performance at  $90^{\circ}\text{C}$ , the highest temperature measured. Figure 3(c) shows the temperature-dependent threshold current density. The characteristic temperature,  $T_0$ , is 112 K between  $20\text{-}50^{\circ}\text{C}$ , and 65 K between  $50\text{-}90^{\circ}\text{C}$ . To further improve the characteristic temperature, p-modulation doped QDs can be applied in future work [2].

#### 4. Conclusions

High performance aluminum-free QD lasers were realized by MOCVD. The maximum WPE is 30%, and the lowest threshold current is 8 mA ( $J_{\text{th}} = 130 \text{ A/cm}^2$ ). Greater than 200 mW single-facet output power was achieved for broad area lasers. These results show promise for providing reliable laser sources for the large-volume datacenter market.

#### 5. Acknowledgements

The authors acknowledge funding support from the Defense Advanced Research Projects Agency (DARPA) Young Faculty Award (YFA) and AIM Photonics.

#### 6. References

- [1] P. G. Eliseev, H. Li, A. Stintz, G. T. Liu, T. C. Newell, K. J. Malloy, and L. F. Lester, "Transition dipole moment of InAs/InGaAs quantum dots from experiments on ultralow-threshold laser diodes," *Appl. Phys. Lett.*, **77**, 262-264 (2000).
- [2] O. B. Shchekin and D. G. Deppe, "1.3 mm InAs quantum dot laser with  $T_0 = 161 \text{ K}$  from 0 to  $80^{\circ}\text{C}$ ," *Appl. Phys. Lett.* **80**, 3277-3279 (2002).
- [3] K. Nishi, K. Takemasa, M. Sugawara, and Y. Arakawa, "Development of quantum dot lasers for data-com and silicon photonics applications," *JSTQE* **23**, 19101007 (1997).
- [4] J. C. Norman, D. Jung, Y. Wan, and J. E. Bowers, "Perspective: The future of quantum dot photonic integrated circuits," *APL Photonics* **3**, 030901 (2018).
- [5] N. T. Yeh, W. S. Liu, S. H. Chen, P. C. Chiu, and J. I. Chyi, "InAs/GaAs quantum dot lasers with InGaP cladding layer grown by solid-source molecular-beam epitaxy," *Appl. Phys. Lett.*, **80**, 535-537 (2002).
- [6] L. Wang, B. Shi, H. Zhao, S. Brunelli, B. Song, D. Oakley, and J. Klamkin, "Toward all MOCVD grown InAs/GaAs quantum dot laser on CMOS-compatible (001) silicon," in *Conference on Lasers and Electro-Optics (CLEO)*, OSA Technical Digest (OSA, 2019), JTu2A.82